Limitations of Voltage Qamp Studies of Slow Inward Current Using the Double Sucrose Gap

R Fischmeister, D Mentrard, G Vassort

Limitations of Voltage Clamp Studies of Slow Inward Current Using the Double Sucrose Gap

R. FISCHMEISTER, D. MENTRARD and G. VASSORT

Laboratoire de Physiologie Cellulaire Cardiaque, U-241, I.N.S.E.R.M., LA 89-3, C.N.R.S., Université de Paris Sud, Bâtiment 443, F 91405 Orsay Cedex, France

Abstract. The electrical behavior of a preparation (single fiber or trabecula) voltage-clamped in a double sucrose gap was checked experimentally on a frog atrial trabecula or using computer simulations. Experimental alterations in isolation factors, maximal inward conductance and series resistance induced unexpected variations in the reversal potential V_{rev} and maximal conductance G_i of slow inward current. Two models were used to examine the conditions required to measure most accurately V_{rev} and G_i. The first model accounted only for longitudinal non-uniformity whereas the second took into account both longitudinal and radial non-uniformities. The two models were compared. With thin preparations a classical single unidimensional model was sufficient to describe the electrical behavior of the preparation. Radial non-uniformity became significant only for preparations with a radius larger than 40 μm. The addition of a diffuse series resistance to the unidimensional model made it applicable to simulate radial non-uniformity of thicker preparations. The unidimensional model was chosen for simulations which revealed several sources of error in the estimation of V_{rev} and G_i. A poor sucrose isolation and the non-uniformity of potential in the test gap appeared most significant; both induce an overestimate of G_i and an underestimate of V_{rev}. These effects can be countered by moderate increases in the series resistance. Furthermore, decreases in slow inward conductance were associated with reductions in the apparent V_{rev}. Variations in the electrical characteristics of the preparation (leak membrane resistance, internal resistances in the different gaps, etc.) can also yield apparent alterations in G_i and V_{rev}. Finally experimental conditions were simulated to reproduce the effects of drugs that alter the slow inward current. The results suggest that V_{rev} (or its variations) cannot easily be determined with accuracy using the double sucrose gap method since its measured value may vary up to 15 mV under given ionic conditions.

Key words: Voltage clamp — Sucrose gap method — Cardiac muscle — Calcium current — Computer simulation

Introduction

Since the double sucrose gap voltage clamp technique was first applied to multicellular preparations (Rougier et al.; 1968; Anderson 1969) several authors have pointed out that current recordings might be distorted by lack of control of membrane voltage (Johnson and Lieberman 1971; Tarr and Trank 1974). Some limitations of the double sucrose gap technique have been explored (Tarr and Trank 1971; Connor et al. 1975) including attempts to monitor the voltage homogeneity with a roving microelectrode (De Hemptinne 1976; Benninger et al. 1976; Tarr and Trank 1976; Horačkova and Vassort 1979; Sauviat 1980). Other investigations have been devoted to determining theoretically whether the current-voltage (I—V) relationships are significantly disturbed by voltage non-uniformities and leakage through sucrose gaps (McGuigan 1974; Ramon et al. 1975; Giles and Noble 1976; Beeler and McGuigan 1978; De Boer and Wolfrat 1979). To our knowledge, none of these authors has examined the conditions required to measure accurately maximal steady state conductance or reversal potential of an inward ionic current (Na, Ca). It was only quoted that changes in the magnitude of the background outward current in a preparation with a large series resistance produce an apparent shift of the reversal potential of an inward current (Connor et al. 1975; Attwell and Cohen 1977). Thus, it is widely held that the reversal potential of the slow inward current can be estimated accurately because near that potential current magnitude is almost negligible. Nevertheless, discrepancies between predicted and measured values of reversal potential of the slow inward current are puzzling. The reported experimental values of reversal potential are low ($V_{rev} \simeq 130$ mV) compared to the expected values assuming that Ca is the only ion flowing through the channel. Drugs that incresase (or decrease) the inward membrane conductance also increase (or decrease) the reversal potential in cardiac tissue of frog (Vassort et al. 1969; Goto et al. 1978; Nargeot et al. 1978), cat (Kohlhardt and Mnich 1978) and rat (Payet et al. 1978). The reported effects on V_{rev} were ascribed to changes in the internal calcium concentration, despite the fact that these changes were opposite to the alterations in amplitude of the current and occurred without simultaneous variations in resting tension.

A single unidimensional cable has often been used to model a unicellular (Moore et al. 1975) or a syncytial preparation(Tomita 1966; McGuigan and Tsien, in McGuigan 1974; Ramon et al. 1975; Giles and Noble 1976) in a double sucrose gap set up. However, radial voltage variations are known to introduce important errors in voltage clamp studies. For example, Haas and Brommundt (1980) showed that the inner cells in a multicellular preparation may fail to achieve adequate voltage control through the intercellular clefts, at least during the early inward current. However, their model is incomplete, since they neglect all sources of distortion other than radial non-uniformity in the test compartment. In

particular their assumption of axial voltage uniformity can not be satisfied at the two test pool sucrose partitions, where external potential gradients are applied to the preparation.

The aim of the present study is to develop two theoretical models simulating the electrical behavior of a voltage clamped preparation in a double sucrose-gap apparatus when both reversal potential V_{rev} and maximal steady state conductance G_i of the slow inward current are measured. The first model, unidimensional, is derived from McGuigan and Tsien (in McGuigan 1974) and includes inward conductance and series resistances. It accounts only for longitudinal variation of membrane potential. The second, radial, accounts for both radial and longitudinal non-uniformity. The determinations of V_{rev} and G_i by the two models are compared. In the present work we also compare experimental results and simulations, and show that changes in some of the parameters characteristic of uni- or multicellular preparation in a double sucrose gap apparatus, can explain apparent variations in reversal potential and maximal steady state conductance.

Methods

Experiments

Voltage-clamp experiments using the double sucrose gap method with vaseline partition (Rougier *et al.* 1968) were performed on sino-auricular trabeculae, 80—120 μm in diameter, isolated from frog (*Rana esculenta*). Test gap was about 150 μm wide and sucrose gap 300 μm. The normal Ringer's solution contained (mmol/l): NaCl, 110.5; KCl, 2.5; $NaHCO_3$, 2.4; $CaCl_2$, 1.8; $MgCl_2$, 1.8; pH 7.4. Temperature: 20 ± 1 °C. Tetrodotoxin (10^{-6} g ml^{-1}) was added during all experiments. Details of alterations of bathing solutions and drug addition are given for each experiment. Voltage clamp experiments were generally carried out with the holding potential equal to the resting membrane potential. In the following description V is the displacement from the resting potential, E_R. Currents were digitized and stored, and the slow inward current analyzed as described later.

Simulations

Calculations were done on a mini-computer system, Plurimat S, Intertechnique. Numerical (unidimensional and radial) models written in FORTRAN IV were accessible to the investigator from an on-line terminal. The mathematical development of these models is detailed elsewhere (Fischmeister 1980) and only most significative equations are given here. The symbols used in these equations as well as the intermediate operators are listed in the glossary.

A. Experimental results

Variations in the apparent reversal potential were determined as a result of, or simultaneously with, variations in the maximal inward conductance in four experimental conditions.

Isolation factors

Under best sucrose isolations, the isolation factor in both gaps was 0.9. In the illustrated experiment (Fig. 1) the initial isolation factors, estimated from the amplitude of the action potentials, were close to 0.85 over both the voltage recording and the current applying gaps. We deliberately decreased the isolation by adding, alternatively to each sucrose gap, a resistance (2.2 MΩ) in parallel. The results are summarized by the two series of three I—V curves obtained with alternation of voltage and current sucrose gaps. A decrease of the isolation factor over the voltage recording gap (S_1) induced a noticeable decrease in the apparent reversal potential (10 mV) while the maximal inward conductance is slightly increased. With the same trabecula the shift in V_{rev} was 6 mV and G_i not significantly changed when the shunt resistance was 3.8 MΩ. A decrease in the isolation factor over the current applying gap (S_2) did not noticeably alter V_{rev} but enhanced 2.5 fold the maximal conductance (1.6 fold in case of 3.8 MΩ).

Conductance

Changes in the maximal inward going conductance, G_i, were produced by allowing for more or less repriming following inactivation by a 80 mV—230 msec depolari-

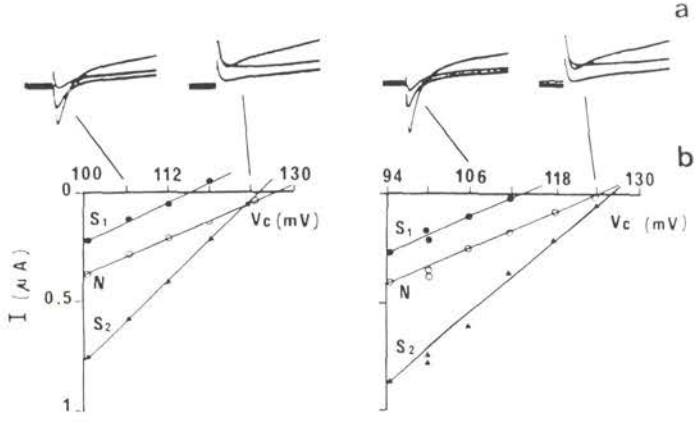

Fig. 1. Alterations in the apparent reversal potential and maximal inward conductance induced by decreasing the isolation factor by a shunt resistance of 2.2 MΩ placed in parallel on the voltage recording sucrose gap (S_1) or the current applying gap (S_2) (with permutation of the two gaps).
a) Current recordings elicited by 106 and 124 mV depolarizations of 200 ms duration.
b) Two series of current-voltage relationships of the maximal inward current for the range of potential in which its slope conductance is linear before and after permutation of the voltage recording and current applying gaps (N, in the absence of a shunt resistance).

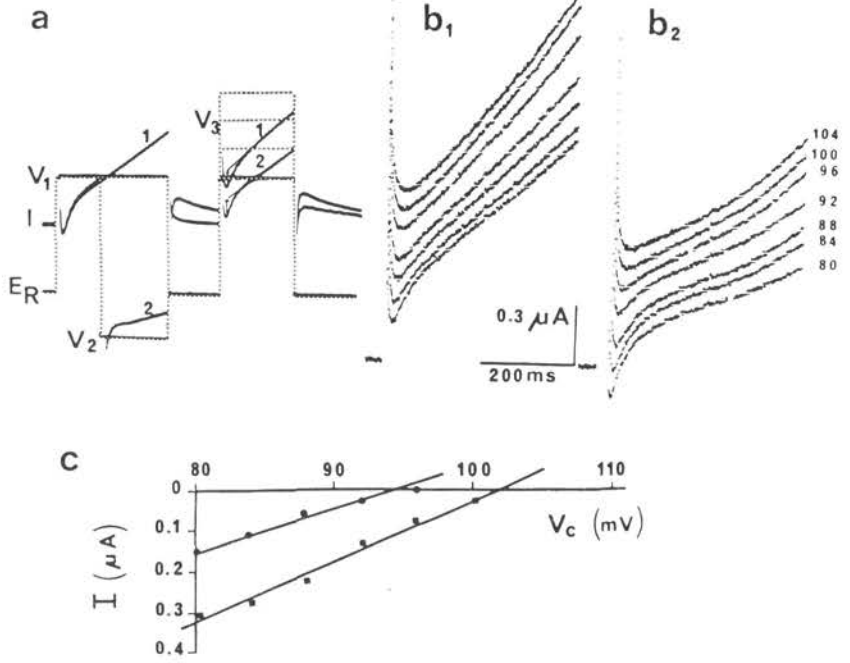

Fig. 2. Decrease in the apparent reversal potential induced by decrease in the inward conductance. a) The two voltage step sequences and the method of estimation of inward current ($V_c = 80$ mV); b_1) and b_2) digitized recordings of currents elicited by increasing V_c from 80 to 104 mV in steps of 4 mV using protocol 1 (●) or 2 (■); c) current-voltage relationships of the maximal inward current obtained following protocols 1 and 2.

zing pulse. Before the test pulse, the membrane was held either at the same potential for further 300 msec (protocol 1) or hyperpolarized to E_r — 30 mV (protocol 2) and in both cases during 270 msec at E_r. This latter membrane polarization allowed for partial repriming in (1) or complemented it in (2). It also resulted in the same capacitive surge making it easier to compare current traces. To minimize the difference in internal Ca concentration between the two protocols and to facilitate current estimation, Li ions were substituted for Na ions to block the Na—Ca exchange and 4-aminopyridine (3×10^{-3} mol/l) and adrenaline (10^{-6} mol/l) were added. Fig. 2 shows the voltage steps and the estimation of inward currents (a) for the two protocols, the original recordings (b) and the resulting I—V relationships (c). The prolonged depolarizations necessary for partial repriming decreased the inward current by about 30% (indicated by the difference in slope of the I—V curves) and increased the outward current. These effects were accompanied by an 8 mV decrease in V_{rev} (from 102 to 94 mV). The

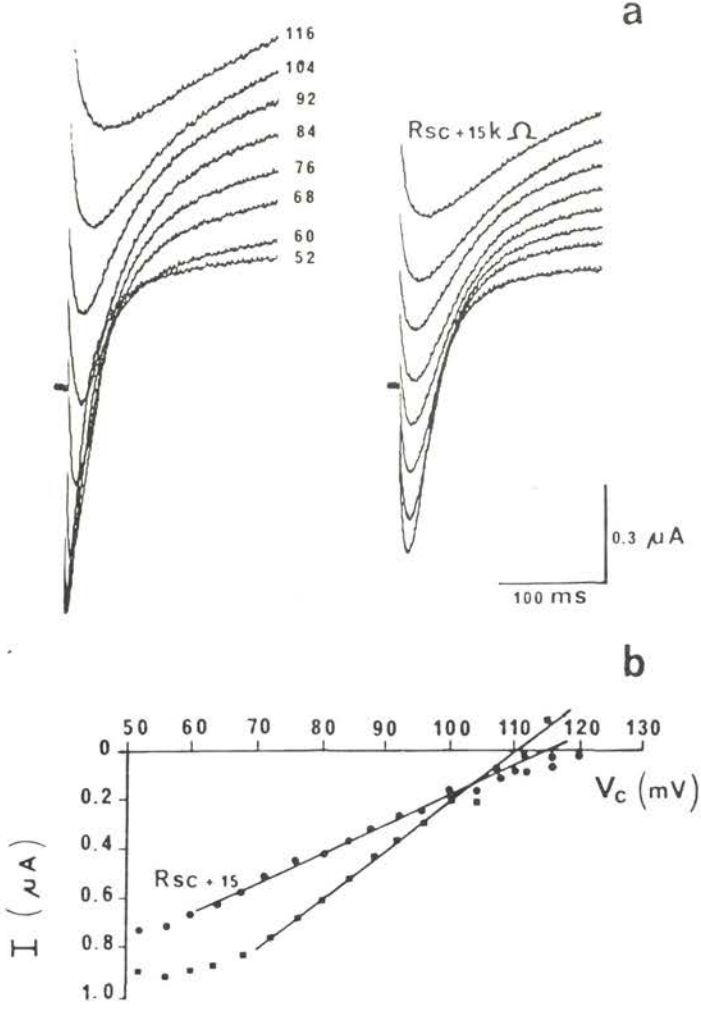

Fig. 3. Effects of the addition of a 15 kΩ series resistance on the maximal inward conductance and the apparent reversal potential: a) digitized recording of currents elicited by the same applied voltages in normal conditions or with a supplementary series resistance electronically added 2 msec after the depolarization; b) current-voltage relationships of the maximal inward current.

low value of V_{rev} resulted (presumably) from the entry of Ca ions during the conditioning pulse and from the Ca-overloading caused by low Na solutions.

Series resistance

A series resistance in the voltage clamp circuit increased the time required to

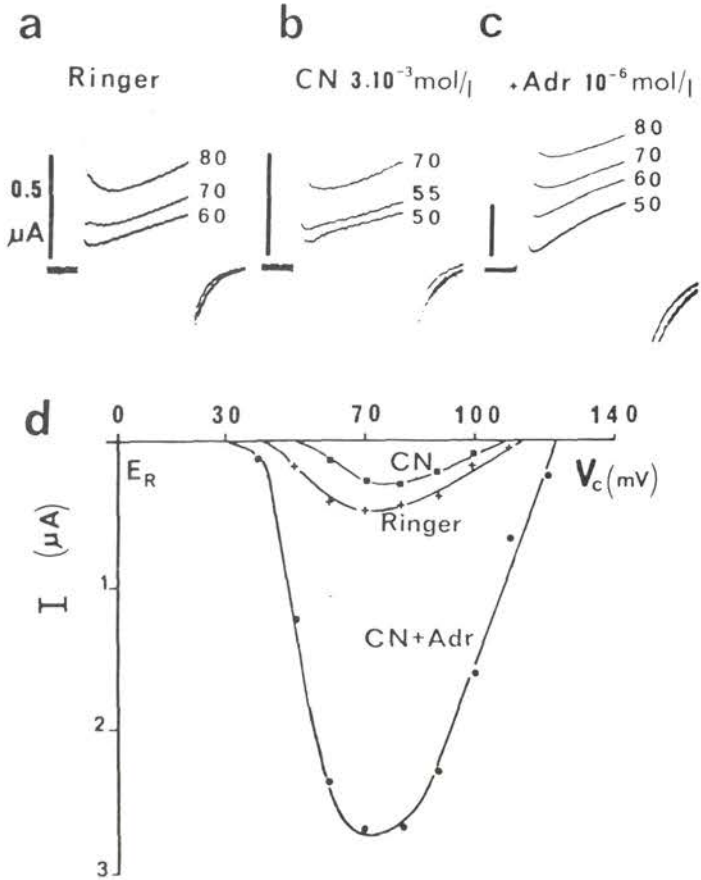

Fig. 4. Effects of cyanide, and adrenaline plus cyanide, on the reversal potential and the maximal conductance of the slow inward current: a) current recordings in Ringer; b) after 20 min of cyanide (3×10^{-3} mol/l) and c) after 4 min following further addition of adrenaline (10^{-6} mol/l). The depolarizing steps (160 msec in duration) were applied from a holding potential of $E_r + 40$ mV. d) Current-voltage relationships of the slow inward currents obtained on another fiber in the same experimental conditions.

charge the membrane capacitance and altered the potential applied to the membrane. In the experimental preparation the common series resistance, R_{sc}, could be varied but not the diffuse series resistance, R_{sd}, which is in the core of the preparation. A 15 kΩ-resistance was electronically added during the depolarizing pulse after a period of 2 msec to allow for charging of most of membrane capacitance. In Fig. 3 (a) are shown the currents elicited by depolarizing pulses in normal conditions or with the additional series resistance, and in 3 (b) the two I—V relationships are drawn. Increasing the series resistance caused a 40% reduction in

the maximal inward and outward conductances, and increased the apparent reversal potential by at least 5 mV. Similar results were obtained in 3 other experiments.

Drug effects

The effects of two drugs, cyanide and adrenaline, known to alter the slow inward conductance in frog heart have been reinvestigated with a particular attention to their effects on the apparent reversal potential. Fig. 4 shows current records elicited by depolarizations applied on top of a holding potential $Hp = E_R + 40$ mV (a) in our standard Ringer's solution, (b) after 20 min in the presence of cyanide (CN, 3×10^{-3} mol/l) and (c) after further 4 min of adding adrenaline (Adr, 10^{-6} mol/l). Current-voltage relationships (d) are given for the maximal inward current obtained with another fibre in the same experimental conditions. In this series of six successful experiments cyanide decreased the inward conductance by 40% and the reversal potential by 9 mV while adrenaline increased the inward conductance by 500% and the reversal potential by 8 mV in average.

B. Theoretical results

1. *Models*
   a) *General Hypothesis*

An idealized double sucrose gap with sharp boundaries between the solutions is considered. In the two external pools, isotonic KCl solution is applied to short circuit the membrane. One is used for recording voltage V_c; current I is applied through the other.

The peak amplitude of the slow inward (or minimal outward) current is measured after graphical substraction of the delayed outward currents. These are extrapolated either linearly (see Horačkova and Vassort 1979; Fig. 5) or exponentially (see Ten Eick et al. 1976; Fig. 1) from the total current elicited after slow conductance had inactivated. The transient capacitive component of current is taken to be zero when the slow component is maximal. This experimental procedure of determining the maximal amplitude of slow inward current was modeled by considering that at each potential any membrane patch in the test node can take only two states: one "active" when the slow conductance reached its peak value and one "passive" when the slow conductance was fully inactivated. Then, the pure inward current I_i can be given by the difference between the two currents obtained in active I_a and passive I_p states. Membrane capacitance is ignored (see discussion).

Since the experimental current-voltage relationship for slow inward current is

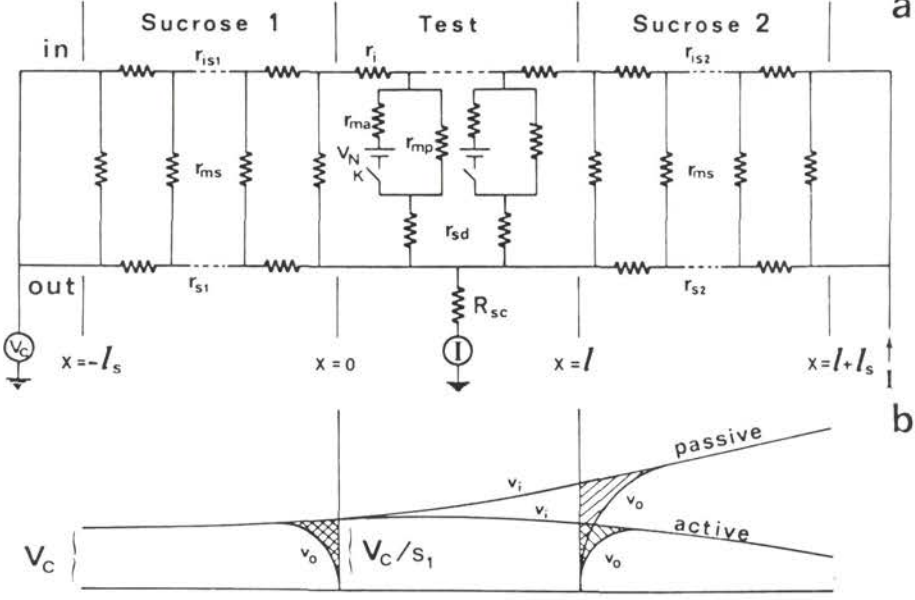

Fig. 5. a) Unidimensional electrical scheme of a preparation set in a double sucrose gap apparatus under voltage clamp conditions. The control potential, V_c, is measured on the left sucrose gap and the current, I, applied on the right sucrose gap. Compartment lengths are l and l_s for test- and sucrose gaps, respectively. Distance x is referred to the idealized partition between test- and sucrose pool on the left side (where $x=0$). Any membrane patch in the test gap can take two states: one passive when the switch "K" is open (as shown), and a second active when the switch K is closed simulating full activation of the slow inward conductance. V_N is the Nernst equilbrium potential and $1/r_{ma}$ is the maximal steady state conductance of slow inward current. r_{ma} and r_{mp} are the membrane resistance in the sucrose gaps and test gap, respectively, $r_{is(1,2)}$ and $r_{s(1,2)}$ are the longitudinal internal and external resistances in the sucrose gaps; r_i, the internal longitudinal resistance, and r_{sd} and R_{sc}, the diffuse and common series resistances in the test compartment. All electrical resistances r are expressed per unit length and can be calculated from specific resistances R using the relations $r(\Omega.\mathrm{cm}^{-1})=R(\Omega.\mathrm{cm})/N\pi a^2$ for longitudinal intra- and extracellular resistance, and $r(\Omega.\mathrm{cm})=R(\Omega.\mathrm{cm}^2)/2N\pi a$ for membrane and series resistances; N and a being respectively the number and the radius of longitudinally orientated fibers.
b) Longitudinal variations of internal, v_i, and external, v_o, potentials during current flow (induced by applying a control potential V_c) for the passive and active states of the preparation. Series resistances were supposed to be nul. Dashed area are proportional to current leak through the sucrose gaps. The isolation factor of the voltage recording sucrose gap S_1 is the ratio $r_{s1}/(r_{s1}+r_{is1})$. The space constant at rest or after the slow inward current has inactivated is $\lambda_p=[(r_{mp}+r_{sd})/r_i]^{1/2}$.

linear in the range of the potentials where the control potential V_c is close to the apparent reversal potential V_{rev}, the active membrane conductance g_{ma} $(=1/r_{ma})$ was set to a constant value. Thus, g_{ma} was in series with a battery, which is assumed to be the Nernst potential for Ca ions, V_N. In the passive state, transmembrane current flows only through the passive membrane conductance g_{mp} $(=1/r_{mp})$. g_{mp}

was also set to a constant value on the assumption that no anomalous rectification occurs in this range of potentials. In the active state, r_{mp} was in parallel with r_{ma} and V_N. All membrane potentials are referenced to the resting potential.

b) *Unidimensional model*

This model was based on the one described by McGuigan and Tsien (in McGuigan 1974), but with added inward currents. An asymmetry in the electrical properties of the three central compartments was also introduced.

The equivalent circuit for the preparation is shown in Fig. 5a. All electrical resistances r are expressed per unit length and could be calculated from specific resistances R using the relations $r = R/N\pi a^2$ for longitudinal intra-and extracellular resistances and $r = R/2N\pi a$ for membrane and series resistances, N and a being respectively the number and the radius of the longitudinally oriented fibers. N is eliminated in the following equations since the unidimensional model is independent of radial dimension. Two types of series resistances have been included in this model: one diffuse, r_{sd}, in series with each membrane segment (Ramon et al. 1975) and one common, R_{sc}, a part of which corresponds to the resistance between the electrode and the bundle surface in the test compartment. These two resistances may be insufficient to account for the cleft resistances in a multicellular preparation unless they can be lumped (Johnson and Sommer 1967). A more realistic representation then requires a continuous variation of the series resistances and can be only provided by a radial model (see later).

The mathematical development of McGuigan and Tsien (in McGuigan 1974) has been used to derive expressions of intracellular and extracellular potentials v_i and v_o as functions of longitudinal distance x in the three compartments (test + two sucrose). Using the intermediate operators Φ and Ψ, general solutions in sucrose pools 1 and 2 are:

$$\Phi = A \sinh (x/\lambda_{s(1,2)}) + B \cosh (x/\lambda_{s(1,2)}) \tag{1}$$

and

$$\Psi = Cx + D\,. \tag{2}$$

In sucrose 1 compartment, C equals zero since no current is applied to this region. The intracellular and extracellular resistances act as a voltage divider and the transmembrane potential V_0 at $x = 0$ is:

$$V_0 = \frac{V_c - R_{sc} I}{S_1}\,. \tag{3}$$

This differs from the control potential V_c even when the common series resistance R_{sc} is set to zero (McGuigan 1974; De Boer and Wolfrat 1979). v_i and v_o are then

given by:

$$v_i = V_0 \left\{ (1 - S_1) \frac{\sinh [(x + l_s)/\lambda_{s1}]}{\sinh (l_s/\lambda_{s1})} + S_1 \right\} + R_{sc} I \tag{4}$$

and

$$v_o = S_1 V_0 \left\{ 1 - \frac{\sinh [x + l_s)/\lambda_{s1}}{\sinh (l_s/\lambda_{s1})} \right\} + R_{sc} I \,. \tag{5}$$

Similar equations for v_i and v_0 may be written in sucrose 2 compartment, except that the current, injected on this side, modifies the boundary conditions.

In the central test pool, the two states, active and passive (see Fig. 5a), of the preparation have to be considered.

— Passive state: according to McGuigan and Tsien (in McGuigan 1974) v_i is in the form:

$$v_i = V_0[\cosh (x/\lambda_p) + B \sinh (x/\lambda_p)] + R_{sc} I_p \tag{6}$$

while v_o is independent of x

$$v_o = R_{sc} I_p \,. \tag{7}$$

A combination of Eq. 3 and of equations describing the continuity of v_i and its derivative dv_i/dx at $x = 0$ and $x = l$ gives an evaluation of the passive current I_p which may be written in the form:

$$I_p = \frac{V_c F(\lambda_p)}{R_{sc} F(\lambda_p) + S_1 S_2 r_{is2} \lambda_p} \,. \tag{8}$$

Because of the series resistance r_{sd}, the membrane potential in the passive state v_{mp} will be only a fraction $f = r_{mp}/(r_{mp} + r_{sd})$ of $v_i - v_o$. Thus,

$$v_{mp} = V_c f S_2 r_{is2} \lambda_p \frac{\cosh (x/\lambda_p) + \lambda_p/\lambda_1 \sinh (x/\lambda_p)}{R_{sc} F(\lambda_p) + S_1 S_2 r_{is2} \lambda_p} \,. \tag{9}$$

When evaluated at $x = 0$:

$$v_{mp}(x = 0) = \frac{V_c f S_2 r_{is2} \lambda_p}{R_{sc} F(\lambda_p) + S_1 S_2 r_{is2} \lambda_p} \,. \tag{10}$$

This expression may be compared to that obtained by McGuigan and Tsien (in McGuigan 1974):

$$v_{mp}(x = 0) = \frac{V_c}{S_1} \,. \tag{11}$$

An equivalent isolation factor S_{eq} may be introduced,

$$S_{eq} = S_1\left(1 + \frac{r_{sd}}{r_{mp}}\right)\left(1 + R_{sc}\frac{F(\lambda_p)}{S_1 S_2 r_{is2}\lambda_p}\right). \tag{12}$$

S_{eq} differs from S_1 because of the non zero series resistances r_{sd} and R_{sc}. S_{eq} is the ratio of control potential V_c to membrane potential at $x=0$ thereby should ideally be 1. From Eq. 12, $S_{eq} \geqslant S_1$, then as long as $S_{eq} < 1$, the presence of series resistances r_{sd} and R_{sc} will tend to reduce the error due to a poor electrical isolation of sucrose solution so that $v_{mp}(x=0)$ is less than expected from Eq. 11.

— Active state: a similar series of equations may be obtained if one considers a Thevenin's representation of a membrane patch. The active equivalent circuit may be deducted from the passive one by replacing r_{mp} by a resistance αr_{ma} in series with a battery αV_N, where $\alpha = r_{mp}/(r_{mp} + r_{ma})$. The length constant is therefore:

$$\lambda_a = \left(\frac{\alpha r_{ma} + r_{sd}}{r_i}\right)^{1/2}. \tag{13}$$

The intracellular potential may be written in the form:

$$v_i = (V_0 - \alpha V_N)\,[\cosh(x/\lambda_a) + B'\sinh(x/\lambda_a)] + \alpha V_N + R_{sc} I_a\,, \tag{14}$$

where the active current I_a is given by:

$$I_a = \frac{V_c F(\lambda_a) - \alpha S_1 V_N G(\lambda_a)}{R_{sc} F(\lambda_a) + S_1 S_2 r_{is2}\lambda_a}. \tag{15}$$

Because of the series resistance r_{sd}, the membrane potential in the active state v_{ma} differs from $v_i - v_o$ as follows:

$$v_{ma} = f'(v_i - v_o) + (1 - f')\alpha V_N \tag{16}$$

where $f' = \alpha r_{ma}/(\alpha r_{ma} + r_{sd})$. While $v_o = R_{sc} I_a$, v_{ma} may be written using Eq. 15 and 16. Thus,

$$v_{ma} = f'[V_c S_2 r_{is2}\lambda_a + \alpha R_{sc} V_N G(\lambda_a)]\,\frac{\cosh(x/\lambda_a) + \lambda_a/\lambda_1 \sinh(x/\lambda_a)}{R_{sc} F(\lambda_a) + S_1 S_2 r_{is2}\lambda_a} +$$
$$+ \alpha V_N[1 - f' \sinh(x/\lambda_a)]\,. \tag{17}$$

Equations describing v_{mp} (9) and v_{ma} (17) may be used to evaluate membrane potential distribution within the test node for the two states of the preparation. Equations of v_i and v_o in sucrose compartments 1 and 2 give longitudinal variations of intra- and extracellular potentials in these pools and the leak current through the sucrose solution can be substracted (Fig. 5b). Eq. 8 and 15 lead to the current-voltage relationship between total recorded ionic current $I_i = I_a - I_p$ and control potential V_c. I_i may be written in the form:

$$I_i = G_i(V_c - V_{rev}) \tag{18}$$

where G_i and V_{rev} are the apparent values of maximal inward conductance and reversal potential, while the true values are $G_{ma} = 1/r_{ma}$ and V_N. Therefore, two correction factors, f_v and f_g, may be introduced as follows:

$$f_v = \frac{V_{rev}}{V_N} \tag{19}$$

and

$$f_g = \frac{G_i}{G_{ma}}. \tag{20}$$

Their complete expressions are given by:

$$f_v = \frac{\alpha G(\lambda_a)[R_{sc}F(\lambda_p) + S_1 S_2 r_{is2}\lambda_p]}{S_2 r_{is2}[\lambda_p F(\lambda_a) - \lambda_a F(\lambda_p)]} \tag{21}$$

and

$$f_g = \frac{r_{ma}}{l}\left[\frac{F(\lambda_a)}{R_{sc}F(\lambda_a) + S_1 S_2 r_{is2}\lambda_a} - \frac{F(\lambda_p)}{R_{sc}F(\lambda_p) + S_1 S_2 r_{is2}\lambda_p}\right]. \tag{22}$$

f_v and f_g may then be used to evaluate separately the influence of each parameter included in our unidimensional model on both determinations of reversal potential, V_{rev} and maximal conductance, G_i of slow inward current.

c) *Radial model*

In this case, the preparation is assumed to be a bundle of fibers (radius A) with a cylindrical symmetry of voltage distribution. Intracellular medium is modeled by an electrically resistive continuum with an effective resistivity R_i. All fibers are considered to have a hexagonal cross section (Adrian et al. 1969). The intercellular space (clefts) in the test pool is filled with a fluid of resistivity ρ_e. Effective external resistivity to radial current flow, R_e is then (Haas and Brommundt 1980):

$$R_e = \rho_e \frac{a\sqrt{3}}{d} \tag{23}$$

where a is the radius of the fibers and d the distance between the surfaces of adjacent fibers. For longitudinal current flow, the effective external resistivity given by the hexagonal model was half the value for radial current flow. However, we considered both resistivities identical which greatly simplified the mathematical model. Thus, extracellular medium may be modeled as a second continuum (Peskoff 1979a and b) electrically coupled to internal space by passive and/or

active membrane resistances (R_{mp}, R_{ma}). For comparison with the unidimensional model, common series resistance R_{sc} was neglected assuming that the outermost layer of fibers in the test gap was at a zero (extracellular) potential. Membrane resistance, R_{ms} and intracellular resistivity, R_{is} in both sucrose gaps were identical and equalled respectively passive membrane resistance, R_{mp} and intracellular resistivity, R_i in the test pool. S was the sucrose isolation factor in either sucrose 1 or sucrose 2 compartment, where the effective extracellular resistivity was R_{es}.

The second order derivatives d^2/dx^2 of the unidimensional model are now replaced by the Laplacian operator in cylindrical coordinates $\Delta = \frac{\partial^2}{\partial x^2} + \frac{1}{r}\frac{\partial}{\partial r}\left(r\frac{\partial}{\partial r}\right)$; r being the distance to the center of the bundle in the radial direction. Differential equations and boundary conditions for Φ and Ψ can be expressed in both sucrose gaps and in the test compartment using, in the active state, the same equivalent membrane patch representation as that used in the unidimensional model.

The mathematical treatment was simplified by using an additional condition placed on the arrangement of electrodes. This condition recognizes that current applied to the bundle in KCl solution was equivalent to that which would have been applied by a disc electrode placed at right angles to the long axis of the preparation, equal to its diameter, at the KCl/sucrose 2 compartment boundary. Similarly potential measured in KCl solution was equivalent to that measured with a disc electrode at the KCl/sucrose 1 compartment boundary. The condition requires also that the preparation, under the sucrose solutions, behaves like a single cell. This latter assumption is justified only when no activity occurs in any fiber of the bundle: this is the case in this part of the preparation since all membranes are in resting state. Then, according to Taylor (1963) and Eisenberg and Johnson (1970), no radial voltage gradient has to be considered when the length constant is larger than the diameter of the preparation. The variation of potential in the two sucrose compartments occurs then only in a direction longitudinal to the fiber axis.

The resolution of the differential equations is based on the study of electrical potential in cylindrical syncitia resulting from an intracellular point source of current (Peskoff 1979b) and is detailed elsewhere (Fischmeister 1980). Relatively simple expressions for passive I_p and active current I_a were derived and could easily be calculated for a given set of electrical properties. As for the unidimensional model, the two correction factors f_v and f_g might be expressed from the total recorded ionic current $I_i = I_a - I_p$.

d) *Comparison between the two models*

The unidimensional and radial models developed above allow two different evaluations of the errors occurring during determinations of both reversal poten-

tial V_{rev} and maximal conductance G_i of the slow inward current. It is thus possible to compare the two models through the correction factors f_v and f_g. Although the unidimensional model is insensitive to the radius A of the cylindrical bundle, the radial non-uniformity of potential can partly be accounted for by the presence of a diffuse series resistance R_{sd}. Results obtained with the radial model for different values of radius A can then be compared to those obtained with the unidimensional model for different values of R_{sd}.

The values of other electrical and morphological parameters of the preparation are referred particularly to frog heart trabeculae. The passive length constant λ_p (5.0×10^{-2} cm) was taken from the literature (Trautwein et al. 1956; Brown et al. 1976; Chapman and Fry 1978). The value of R_i (588 Ω.cm) is given by Chapman and Fry (1978) and R_{mp} (11.76 KΩ.cm^2) was then calculated from λ_p and R_i, assuming a 2.5 μm radius a for each fiber. The cleft width d (3×10^{-6} cm) and the resistivity ϱ_e(83.3 Ω.cm) of the extracellular fluid were taken as in Haas and Brommundt (1980) leading to a high effective resistivity R_e (12.02 KΩ.cm). For both models a perfect symmetry was considered between internal resistivities and passive membrane resistances in all compartments ($R_{is1} = R_{is2} = R_i$ and $R_{ms} = R_{mp}$). The isolation factors (S_1, S_2) were assumed identical in both sucrose gaps and equal to 0.9. It results that with the unidimensional model the control potential V_c is only 90 per cent of the potential actually applied to the membrane at the left boundary of the test gap (McGuigan and Tsien, in McGuigan 1974; Fig. 5b). The active conductance was chosen two times larger than the passive one, and the true reversal potential V_N was set at 160 mV. Three different values of the test gap length l were considered because this parameter plays a predominant role (through the ratio l/λ_p) in the longitudinal voltage non-uniformity. l_s is taken sufficiently higher than l and the common series resistance R_{sc} is set at zero.

Calculated values of f_v and f_g are shown in Table 1. For three values of the test compartment length ($l = 100$, 200 and 300 μm) f_v and f_g were calculated with the unidimensional model considering a diffuse series resistance nul or 580 Ω.cm^2, or with the radial model for $A = 20$, 40 or 80 μm. Results obtained either with unidimensional or radial model showed that $f_v < 1$ and $f_g > 1$. Measurement conditions were improved when l was decreased since f_v increases and f_g decreases, but no optimal conditions were found (see later). Thus, with both models, the reversal potential V_{rev} was always underestimated and the maximal conductance G_i overestimated. Adding series resistance R_{sd} to the unidimensional model, or increasing the diameter of the preparation in the radial improved both determinations of V_{rev} and G_i. Results obtained with either unidimensional or radial models of a preparation with a small radius ($A = 20$ or 40 μm) were similar. Besides, for larger preparations ($A = 80$ μm), values of f_v obtained with the radial model could be accurately fitted by the unidimensional model when a 580 Ω.cm^2 series resistance R_{sd} was added. In this case, values of f_g obtained with the unidimensional

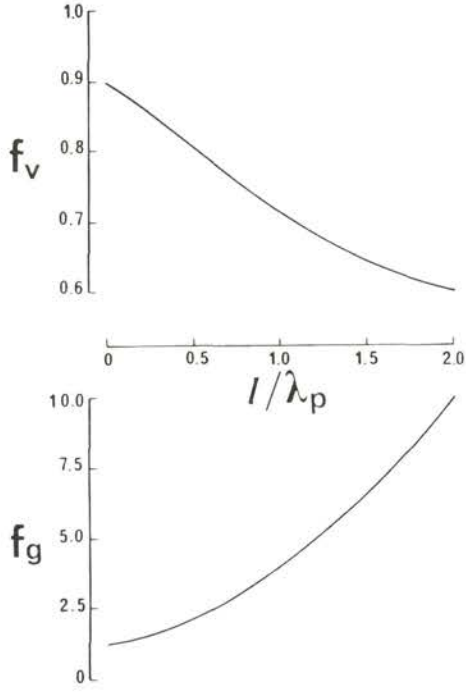

Fig. 6. Dependence of the correction factors f_v and f_g (ratios of estimated to real values of the reversal potential and the maximal conductance) on the electrotonic distance l/λ_p, when either l or λ_p is modified.

model are slightly higher than those obtained with the radial model. Thus, radial inhomogeneity is not significant in small preparations and is equivalent to a series resistance added to a unidimensional cable model.

2. *Simulations*

Following the above conclusions the unidimensional model was selected to analyse the consequences of alterations in different parameters on the determination of both the apparent reversal potential V_{rev} and the maximal inward conductance G_i. The variations were quantified by the two correction factors f_v ($= V_{rev}/V_N$) and f_g ($= G_i/G_{ma}$).

a) *Parameters related to the test gap*

Electrotonic distance: l/λ_p

The electrotonic distance depends on both the preparation and the experimental set up. If has often been recognized as an important factor that determines potential non-uniformity during voltage clamp experiments. Usual values range between 0.2 (Tarr and Trank 1971) and 0.6 (Brown *et al.* 1976). Large values of l/λ_p (0.6—0.9) have been shown to minimize the relative contribution of the leakage current to the total current (McGuigan and Tsien, in McGuigan 1974). This is justified for outward currents but should be reconsidered for inward currents. Fig. 6 shows the effects of electrotonic distance on f_v and f_g as either l or λ_p are altered. It appears that f_v is always less than 1 while f_g is greater than 1 and that both differences from unity increase with l/λ_p. This implies that the reversal potential V_{rev} is always underestimated and the active conductance G_i overestimated. Furthermore, except when $l/\lambda_p \ll 1$, f_v is always less than S_1^0 (i.e. 0.9); thus the reversal potential is underestimated even more than the control potential.

Since degree of voltage uniformity in the test gap determines the accuracy of voltage clamp studies, f_v and f_g were calculated for three different test gap lengths giving values of 0.2, 0.4 and 0.6 for the initial electrotonic distance. For these three increasing values of l/λ_p^o and for the other parameters at their initial state it was possible to calculate the two correction factors f_v and f_g for the beginning of any experiment: $f_v = 0.87$, 0.83 and 0.79; $f_g = 1.35$, 1.55 and 1.83.

Active membrane conductance: G_{ma}

The dependences of f_v and f_g on the relative variation of G_{ma} are reported in Fig. 7a. Both f_v and f_g increase with G_{ma}/G_{ma}^o, the variations being more marked with large values of l/λ_p^o. The increase in f_v, towards values close to S_1^o, suggests that a better estimation of V_{rev} may be possible with large values of active conductance. It implies variations of the estimated reversal potential even when only the active conductance is altered. The increase in f_g indicates that the conductance will be increasingly overestimated as G_{ma} and l/λ_p^o increase. These results extend those of Giles and Noble (1976) who considered a perfect isolation in both sucrose compartments.

Under voltage clamp conditions the maximal active slow membrane conductance may be up to 20 times the value of passive membrane conductance. This should correspond to large variations of f_v and f_g when the active conductance is altered by external agents. This is emphasized in Fig. 7b which shows reconstructions of I—V curves put in legend only for three values of G_{ma}/G_{ma}^o. Everything

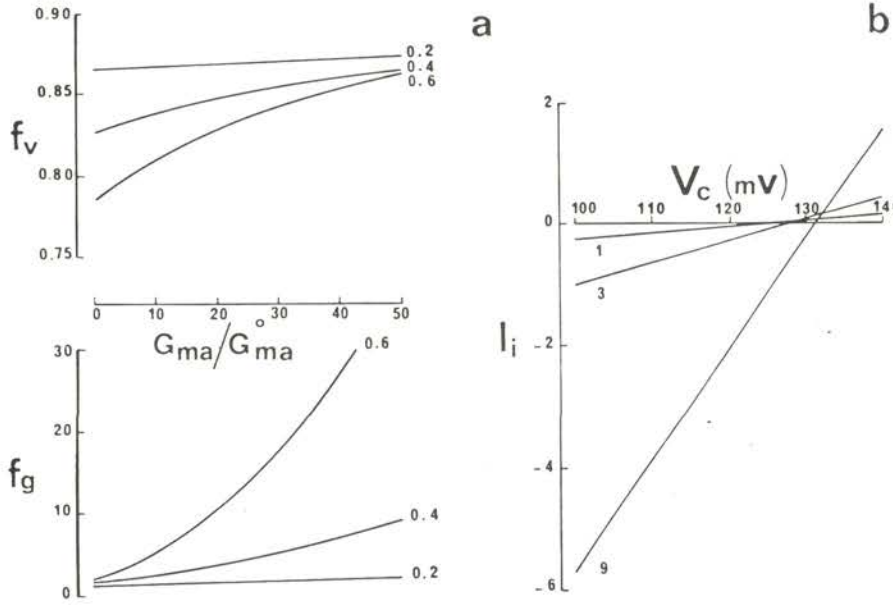

Fig. 7. a) Dependence of f_v and f_g on G_{ma}/G^o_{ma}, the maximal active conductance relative to its initial value, for three different values of the test gap length so that $l/\lambda^o_p = 0.2$, 0.4 and 0.6. b) Reconstruction of I—V curves for three different values of G_{ma}/G^o_{ma}: 1, 3 and 9, when $l/\lambda^o_p = 0.6$. I_i in arbitrary unit (for details see text).

else being constant the larger the inward conductance the higher the reversal potential.

Internal resistance and passive membrane resistance: R_i, R_{mp}

Modifications in R_i and R_{mp} can result from changes in external and/or internal medium. Changes in internal resistance are mostly due to alterations in intercellular junctions and have been attributed to an increase in the intracellular Ca concentration (De Mello 1975; Weingart 1977; Loewenstein et al. 1978) or to a decrease of pH (Turin and Warner 1977). Recent works have described a marked increase in R_i under anoxia (Payet et al. 1978) or hypoxia (Wojtczak 1979). The reported variations of R_{mp} are opposite: Meech (1974) and Isenberg (1977) observed a decrease of R_{mp} when increasing the intracellular Ca concentration, and Payet et al. (1978) measured a 44 percent decrease of R_{mp} within 20 min of anoxia.

In Fig. 8 are shown the variations of f_v and f_g under specificic alterations in R_i and R_{mp}. The first alterations (Fig. 8a) is to assume an asymmetry between the three internal resistances; the second (Fig. 8b) is to introduce a modification of the relative value of the active conductance with respect to the passive one. Both R_i

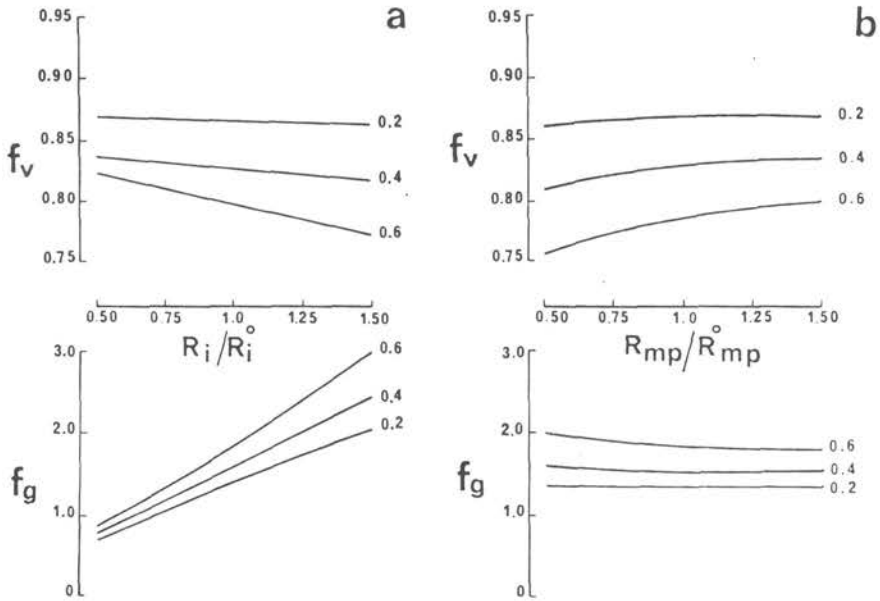

Fig. 8. Dependence of f_v and f_g on the relative values of internal resistivity R_i/R_i^o (a) and passive membrane resistance in the test gap R_{mp}/R_{mp}^o (b) for $l/\lambda_p^o=0.2$, 0.4 and 0.6.

and R_{mp} control the length constant. An increase in R_i as well as a decrease of R_{mp} induces a decrease of f_v and an increase in f_g. Since under experimental conditions the variations of R_i and R_{mp} are opposite, their effects on f_v and f_g will be cumulative. Moreover, if changes in R_i and R_{mp} are due to variations of the internal calcium concentration a non-constant V_N should be introduced. Thus a larger shift of V_{rev} would be induced since f_v and V_N vary in the same direction.

b) *Parameters related to the sucrose gaps*

Isolation factors: S_1, S_2

Only those variations in S_1 and S_2 that result from changes in $R_{s(1,2)}$ are considered. Since one can assume that $R_{s(1,2)}$ remains constant during an experiment (except for the first few minutes), the variations reported here may correspond to different initial conditions concerning the sucrose isolation. For a single cell the value of $S_{(1,2)}$ is close to 1 (within 5%) (Julian et al. 1962) but for multicellular preparations $S_{(1,2)}$ is never greater than 0.9 and is sometimes as low as 0.7 (New and Trautwein 1972).

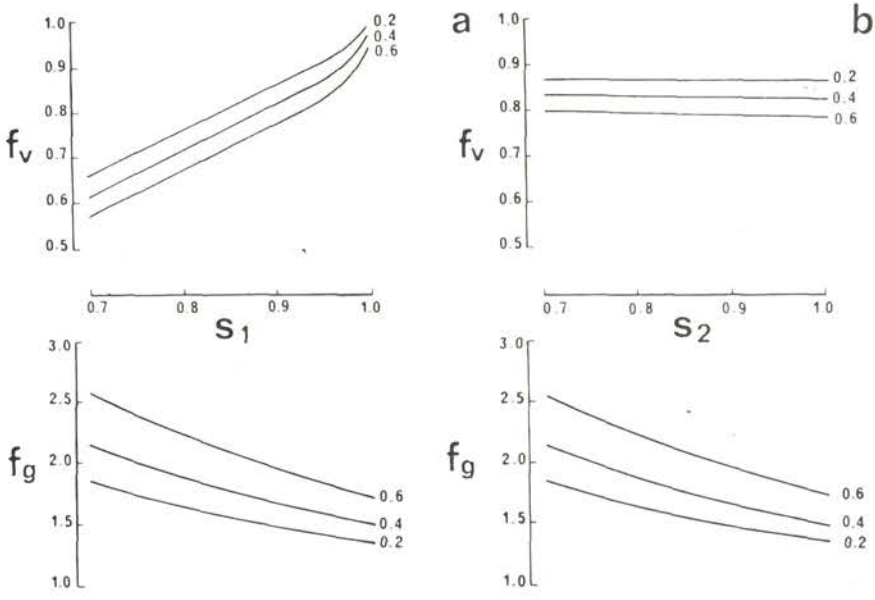

Fig. 9. Dependence of f_v and f_g on the isolation factors S_1 (a) and S_2 (b) for $l/\lambda_p^o = 0.2$, 0.4 and 0.6.

The influence of $S_{(1,2)}$ on the two correction factors, f_v and f_g, is shown in Fig. 9 (a and b). It appears that f_v increases with S_1 but remains smaller than S_1. f_v is almost unaltered by changes in S_2. f_g is greater than 1 and is similarly decreased by increasing values of S_1 and S_2.

Internal resistances: R_{is1}, R_{is2}

Variations in the internal resistances, R_{is1} and/or R_{is2}, relative to the initial value $R_{is1}^o = R_{is2}^o = R_i^o$, alter S_1 and S_2 but also induce an asymmetry between the 3 gaps. Their effects on f_v and f_g are shown in Fig. 10 (a and b) together with the alterations in $S_{(1,2)}$ for comparison with the specific effects of $S_{(1,2)}$ reported in Fig. 9. Surprisingly, it appears that following modification of R_{is2}, the variation of f_g is opposite to that expected from the alteration in S_2. This is due to a change in the voltage drop across R_{is2} when current is injected. Such variations in the internal resistances may occur during an experiment. It has been reported (Kléber 1973) that the internal resistance under the sucrose solution increases exponentially by ten times in four hours i.e. more than 20 percent in the first 20 min. The increase may be even larger in the gap through which the current is injected. Thus, one can expect a decrease with time of apparent reversal potential unrelated to variations of the internal Ca concentration.

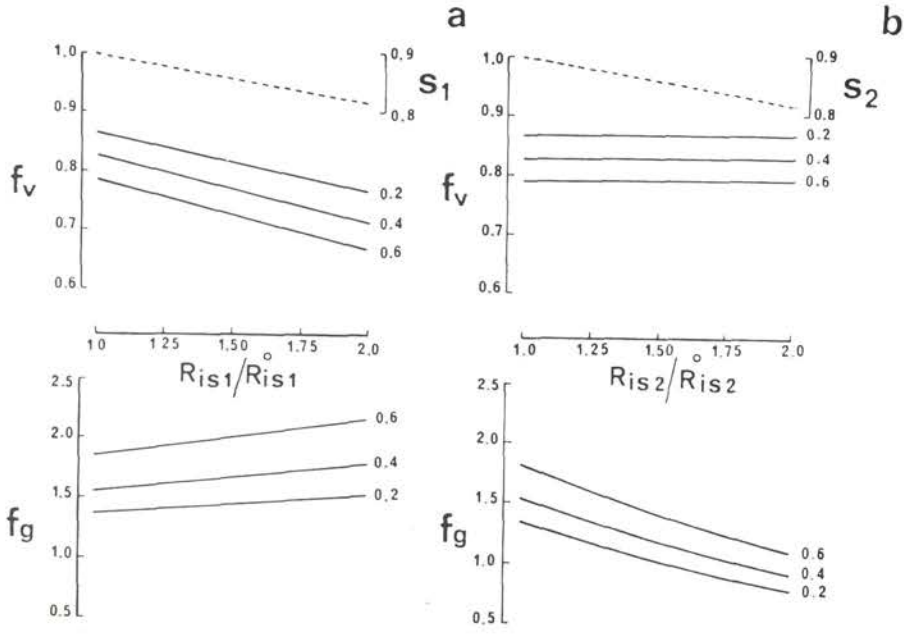

Fig. 10. Dependence of f_v and f_g on the relative values of internal resistivities in the two sucrose compartments R_{is1}/R^o_{is1} (a) and R_{is2}/R^o_{is2} (b) for $l/\lambda^o_p = 0.2$, 0.4 and 0.6. Simultaneously the consequent variations of the two isolation factors, S_1 and S_2 are reported in the upper curves.

Membrane resistance and length of the sucrose gaps: R_{ms}, l_s

The length constant in the two sucrose gaps is $\lambda_{s(1,2)} = \{r_{ms}/[r_{is(1,2)} + r_{s(1,2)}]\}^{1/2}$ and equals $[1 - S_{(1,2)}]^{1/2}\lambda_p$ (i.e. 1.58×10^{-2} cm) in our initial conditions. In ideal case the electrotonic distance should be $l_s/\lambda_{s(1,2)} \gg 1$ (McGuigan and Tsien, in McGuigan 1974). This might be difficult to achieve when the passive length constant of the tissue is in the order of a few millimeters (e.g. more than 2 mm in sheep Purkinje fibers; Bonke 1973) or when the sucrose isolation $S_{(1,2)}$ is poor. Furthermore R_{ms} may increase during the experiment (Kléber 1973) which would result in an increase in $\lambda_{s(1,2)}$. However the model shows that only a small error (a few percent) is introduced when the electrotonic distance in the sucrose gaps is close to 1.

c) *Influence of series resistances:* R_{sd}, R_{sc}

The usual values reported in the literature of R_{sd} range between 0.02 to 0.06 times the passive membrane resistance (Beeler and Reuter 1970; Connor et al. 1975; De Hemptinne 1976) while R_{sc}, calculated for a unit membrane area, is generally lower (Attwell and Cohen 1977). The variations of the two correction factors f_v

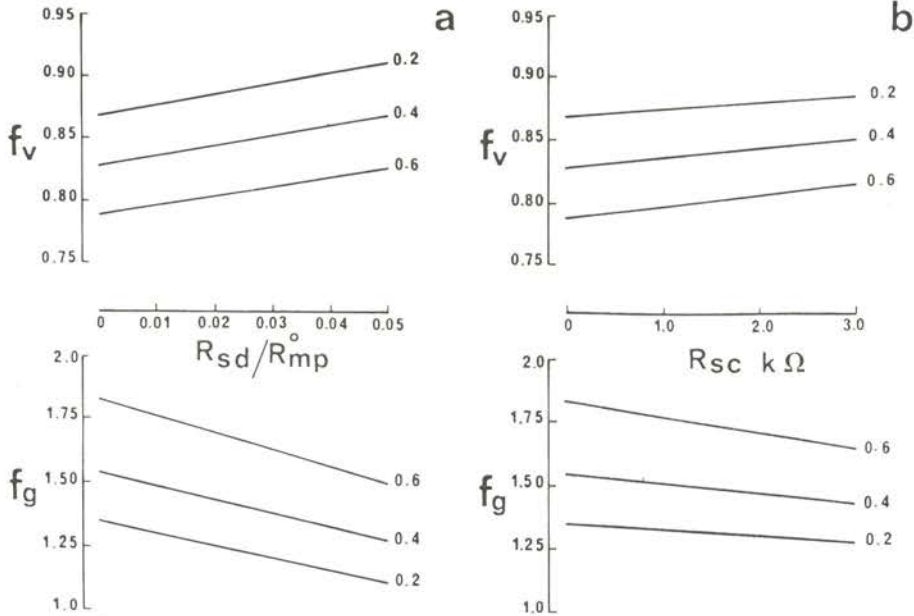

Fig. 11. Dependence of f_v and f_g on the two series resistances R_{sd} (a) and R_{sc} (b) for $l/\lambda_p^o = 0.2$, 0.4 and 0.6. R_{sd} is expressed relatively to the passive membrane resistance R^o_{mp}.

and f_g with alterations in the two series resistances R_{sd} and R_{sc} are shown in Fig. 11 (a and b). An increase in either R_{sd} or R_{sc} increases f_v and decreases f_g. Thus the series resistances tend to reduce the errors caused by the other parameters in both determinations of reversal potential and conductance. This compensation is due to opposite effects of longitudinal gradient and series resistances on voltage uniformity. Such a fact has been already pointed out by Ramon et al. (1975) though they did not simultaneously study the two effects on current-voltage relationships. The model shows that both series resistances increase the equivalent isolation factor S_{eq} (Eq. 12) and furthermore that R_{sd} extends the length constant λ_p. Both effects tend to improve the measurement conditions.

d) *Applications to drug effects*

To compare with the experimental results reported in Fig. 4 the effects of drugs that alter inward membrane conductance were simulated assuming they do not modify the true reversal potential. While the inhibitory effect of cyanide was maximal within 20 min, the stimulatory effect of adrenaline was quasi instantatenous. Two series of I—V curves obtained for two electrotonic distances are reported (Fig. 12). As parameters other than G_{ma} were also influenced by the drugs

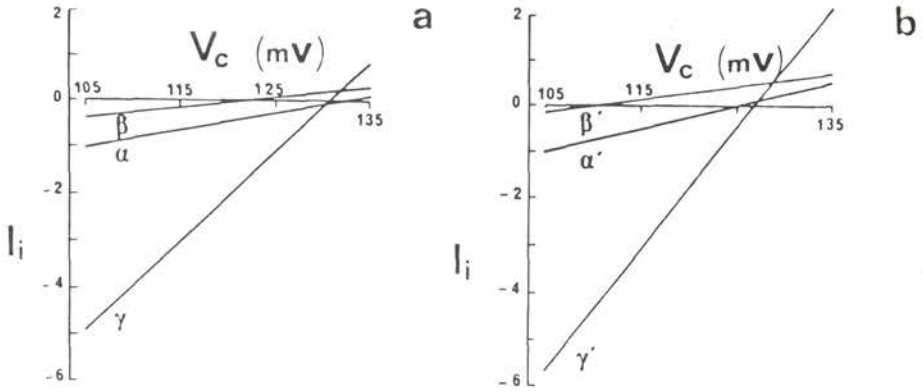

	Curve	$\frac{R_{is}}{R_{is}^{o}}$	S	$\frac{R_i}{R_i^{o}}$	$\frac{R_{mp}}{R_{mp}^{o}}$	$\frac{G_{ma}}{G_{ma}^{o}}$	V_N	$\frac{G_i}{G_i^{o}}$	V_{rev}
							mV		mV
a	α	1.0	0.90	1.0	1.0	1.0	160	1.0	132
$l/\lambda_p^o = 0.4$	β	1.2	0.88	1.5	0.5	0.4	–	0.6	122
	γ	1.2	0.88	0.5	1.5	10.0	–	5.1	131
b	α'	1.0	0.90	1.0	1.0	1.0	160	1.0	125
$l/\lambda_p^o = 0.6$	β'	1.2	0.88	1.5	0.5	0.3	–	0.6	111
	γ'	1.2	0.88	0.5	1.5	9.0	–	5.2	127
						real		estimated	

Fig. 12. Simulations of the effects of cyanide (β and β') and adrenaline (γ and γ') on the estimated values of reversal potential V_{rev} and maximal conductance G_i of slow inward current (α and α': initial conditions) for two values of l/λ_p^o: 0.4 (a) and 0.6 (b). I_i in arbitrary unit. In the Table are listed the values of the selected parameters used in the simulation. The real value of revesal potential, V_N, was constant and the relative variations of maximal conductance, G_{ma}/G_{ma}^o, were chosen to obtain relative variations of the estimated conductance, G_i, G_i^o, close to those observed experimentally.

and the duration of the experiment, their variations in Fig. 12 were also included in the simulation (see Table 1). Series resistances were not taken into account since the diameter of the preparations we used were close to 80 μm for which we have shown that the effect of diffuse series resistance can be neglected, and we suppose the common series resistance was electronically compensated.

Assuming l/λ_p^o to be respectively 0.4 (Fig. 12a) and 0.6 (Fig. 12b), a 40% decrease in G_i during simulation of CN effects is obtained by decreasing G_{ma} by 60 or 70% respectively. This occurs together with a diminution of 10 and 14 mV of V_{rev}. These values are in the range of those observed in Fig. 4 and reported by others (Nargeot et al. 1978; Kohlhardt and Mnich 1978; Ventura-Clapier and Vassort 1980).

Table 1. Comparison of the correction factors for the reversal potential f_v and maximal conductance f_g of the slow inward current obtained for three test-gap lengths with the unidimensional model without or with a diffuse series-resistance and with the radial model considering three different radii of the preparation.

	Unidimensional model				Radial model					
	$R_{sd}=0$		$R_{sd}=580\ \Omega cm^2$		$A=20\times10^{-4}$ cm		$A=40\times10^{-4}$ cm		$A=80\times10^{-4}$ cm	
l µm	f_v	f_g	f_v	f_g	f_v	f_g	f_v	f_g	f_v	f_g
300	0.79	1.82	0.83	1.43	0.78	1.83	0.79	1.62	0.83	1.30
200	0.83	1.54	0.87	1.26	0.83	1.60	0.84	1.44	0.88	1.17
100	0.87	1.35	0.91	1.11	0.87	1.48	0.88	1.33	0.92	1.09

Therefore the apparent diminution of V_{rev} should not necessarily be attributed to an increase in the internal calcium concentration. On simulating the addition of adrenaline to cyanide V_{rev} approximatively recovers its value in Ringer solution if G_{ma} increased by 9 or 10 fold, an increase necessary to account for the 5 fold measured increase in G_i. Since experimentally the values of V_{rev} are 5 to 10 mV higher in adrenaline than in Ringer a real decrease of the intracellular Ca concentration might be considered in this case.

Discussion

Although a unidimensional cable has often been used to model the electrical behavior of multicellular preparations (Tomita 1966; McGuigan and Tsien, in McGuigan 1974; Jack et al. 1975; Ramon et al. 1975), such representations are not sufficient to account for the transient charging of membrane capacitance, since during that period the extracellular resistance to radial current flow is the major resistive determinant of the membrane capacitive response. As shown by Jakobsson et al. (1975), a distribution of extracellular resistances and membrane capacitances in the cross section leads then to a much more realistic representation. A model concerned solely with the influence of radial non-uniformities upon the current records, obtained with a double sucrose gap, is justified for studying the capacitive transient and the fast sodium current in a multicellular preparation (Jakobsson et al. 1975; Haas and Brommundt 1980) but may be inadequate to represent other slower or delayed currents. The present study shows that, at least during the slow inward current, the influence of longitudinal non-uniformity upon the voltage clamp records becomes predominant in a double sucrose gap set up. The particular application we have had in mind is to determine the reversal potential and maximal conductance of the slow inward current for cardiac

preparations. Comparison between results obtained with a classical unidimensional model and with a model accounting for both radial and longitudinal variations of potential leads to the following conclusions: i) radial voltage non-uniformity during the slow inward current becomes significant only for preparations with large radius ($A > 40$ μm for frog heart), ii) for thin preparations, a classical single unidimensional model is sufficient to describe the electrical behavior of the preparation, iii) the addition of an adequate diffuse series resistance to this model makes it applicable to simulate radial non-uniformity of larger preparations.

The most important errors in the determinations of V_{rev} and G_i arise from longitudinal non-uniformity of potential in the test gap (Fig. 6) and from poor isolation in the sucrose gaps (Fig. 1 and 9 a—b). Optimal conditions can be found only by decreasing the test gap length. Nevertheless, with $l/\lambda_p = 0.2$ most of our curves still show some sensitivity to variations of specific parameters and a non negligible error remains in the determinations of both V_{rev} and G_i. Our results confirm and extend the works of McGuigan and Tsien (in McGuigan 1974) and De Boer and Wolfrat (1979). Our correction factor f_g, for an inward going conductance, should be compared to the correction factor q of the first authors for the outward going conductance, for which they showed an optimal electrotonic distance of about 0.9.

The apparent reversal potential of inward currents has long been considered as that potential at which there was no difference between the applied and the true membrane potential notwithstanding the presence of a series resistance (Ramon et al. 1975). However, Attwell and Cohen (1977) suggested that an increase in the outward conductances, attributable to G_{mp}, could increase the apparent reversal potential of the related current. In both our model (Fig. 7) and our experimental observations (Fig. 2) a decrease in G_{ma} or an increase in G_{mp} reduces the apparent reversal potential. This results from an enhancement of the longitudinal non-uniformity which is the main cause of the underestimate of V_{rev}. Our experimental and computed data (Fig. 3 and 11) also show that the series resistance (independent of capacitance charge) alters V_{rev}. This is due to the cable properties of the preparation and the imperfect isolation of the central compartment by the two sucrose gaps. To test the second factor, Ramon et al. (1975) introduced in their model a shunt resistance, accounting for the leak current in the sucrose gap through which the current is applied. The lack of effect on the reversal potential together with the increase in the maximal conductance (of the sodium current) are compatible with the above variations in f_v and f_g induced by altering S_2 (Fig. 1 and 9b). The direct effects of series resistances on V_{rev} are negligible because the magnitude of the slow conductance is small (Reuter and Scholz 1977). However the unidimensional model shows that in the case of large series resistances the effects of variations in other parameters are attenuated while they are amplified with preparations of small diameter in which the specific series resistances tend

towards zero. Furthermore the effects of series resistances in relation with the membrane capacitance may also be neglected. First the time constant of slow channel activation is large, compared with the time constant of capacitance charge and the above protocols allow to bring into comparison currents elicited by the same voltage steps applied in different conditions. Secondly, the radial non-uniformity induced by membrane capacitance is small at peak activation of slow inward channel (Kass et al. 1979; Schoenberg and Fozzard 1979); indeed, this factor is even smaller with the double sucrose gap than with the microelectrode method, since we show that the radial component is less important. Thus the addition of a membrane capacitance to the model is not required.

One inference of the present study is that, with the double sucrose gap voltage clamp method, the reversal potential V_{rev} of the slow inward current is underestimated whereas the maximal steady state conductance G_i is overestimated. The relatively low experimental value for the reversal potential in cardiac tissues, by comparison to the value calculated from Nernst potential for the Ca^{2+} ions, may not be due only to imperfect selectivity of the slow inward channel, as suggested by Reuter and Scholz (1977). Other implications of the present work concern the variations of V_{rev} and G_i recorded during an experiment which may be the results of modifications in other parameters than the internal ionic concentration and channel conductance. Indeed any alteration in the passive characteristics of a preparation, induced by drugs or duration of experiment, will modify the apparent active conductance and reversal potential. To be valid a physiological interpretation requires the control of all electrical and morphological parameters of preparations set in the experimental apparatus.

Acknowledgement. We thank Dr R. De Boer for helpful advice and Prof. R. L. De Haan for stimulating discussions and for reading the manuscript. The technical assistance of the Laboratoire de Physiologie Comparée, particularly of Mrs P. Richer, is gratefully acknowledged.
This work was supported by grants from D.G.R.S.T. (BFM 78 7 2584) and I.N.S.E.R.M. (CRL 77 1 012 5).

Glossary

Unidimensional model

x	longitudinal coordinate (cm).
l, l_s	length of test, sucrose compartments (cm).
R_i, r_i	intracellular resistivity in test compartment (Ω.cm), (Ω.cm^{-1}).
$R_{is(1,2)}$, $r_{is(1,2)}$	intracellular resistivity in sucrose (1,2) compartments (Ω.cm), (Ω.cm^{-1}).

$r_{s(1,2)}$	extracellular resistivity in sucrose (1,2) compartments ($\Omega.\mathrm{cm}^{-1}$).
$S_{(1,2)} = r_{s(1,2)}/(r_{s(1,2)} + r_{is(1,2)})$	isolation factors of sucrose (1,2) compartments (dimensionless).
$R_{m(p,a)}$, $r_{m(p,a)}$	membrane resistance (passive, active) in test compartment ($\Omega.\mathrm{cm}^2$), ($\Omega.\mathrm{cm}$).
R_{ms}, r_{ms}	membrane resistance in sucrose compartments ($\Omega.\mathrm{cm}^2$), ($\Omega.\mathrm{cm}$).
R_{sd}, r_{sd}	diffuse series resistance ($\Omega.\mathrm{cm}^2$), ($\Omega.\mathrm{cm}$).
R_{sc}	common series resistance (Ω).
$\lambda_p = [(r_{mp} + r_{sd})/r_1]^{1/2}$	length constant in passive state in test compartment (cm).
λ_a (Eq.13)	length constant in active state in test compartment (cm).
$\lambda_{s(1,2)} = [r_{ms}/(r_{is(1,2)} + r_{s(1,2)})]^{1/2}$	length constant in sucrose (1,2) compartments (cm).
v_i, v_o, v_m	intracellular, extracellular and transmembrane potential (mV).
V_0, V_l	transmembrane potential at both sides of the test compartment (mV).
v_{mp}, v_{ma}	transmembrane potential in passive and active state in test compartment (mV).
I (I_a or I_p)	total current, active or passive (mA).
I_i (Eq.18)	net slow inward current (mA).
G_i, $G_{ma}(= l/r_{ma})$	apparent and true total maximal inward conductance (Ω^{-1}).
V_{rev}, V_N	apparent reversal potential or Nernst potential of slow inward current (mV).
S_{eq} (Eq.12)	equivalent isolation factor (dimensionless).
f_v (Eq.19), f_g (Eq.20)	correction factors for the reversal potential or the maximal conductance (dimensionless).

Radial model

R_e, ϱ_e	effective and specific extracellular resistivity in test compartment ($\Omega.\mathrm{cm}$).
A, a	radius of the trabeculae, of one fiber (cm).
d	distance between two adjacent fibers (cm).
r	distance to the center of the bundle in radial direction (cm).

Intermediate operators

Φ	$= v_i - v_o$.
Ψ	$= v_i + \beta v_o$.
β	ratio of intra- to extracellular resistivity in the different compartments (dimensionless).
$\frac{1}{\lambda_{(1,2)}}$	$= \frac{1 - S_{(1,2)}}{\lambda_{s(1,2)}} \coth (l_s/\lambda_{s(1,2)})$.
$F(\lambda)$	$= \lambda\left(\frac{1}{\lambda_1} + \frac{1}{\lambda_2}\right) \cosh (l/\lambda) + \left(1 - \frac{\lambda^2}{\lambda_1 \lambda_2}\right) \sinh (l/\lambda)$.
$G(\lambda)$	$= \frac{\lambda}{\lambda_2} [\cosh (l/\lambda) - 1] + \sinh (l/\lambda)$.

References

Adrian R. H., Chandler W. K., Hodkin A. L. (1969): The kinetics of mechanical activation in frog muscle. J. Physiol. (London) **204,** 207—230

Anderson N. C. (1969): Voltage clamp studies on uterine smooth muscle. J. Gen. Physiol. **54**, 145—165

Attwell D., Cohen I. (1977): The voltage clamp of multicellular preparations. Progr. Biophys. Mol. Biol. **31**, 201—245

Beeler G. W., McGuigan J. A. S. (1978): Voltage clamping of multicellular cardiac preparation: capabilities and limitations of existing methods. Progr. Biophys. Mol. Biol. **34**, 219—254

Beeler G. W., Reuter H. (1970): Voltage clamp experiments on ventricular myocardial fibres. J. Physiol. (London). **207**, 165—190

Benninger C., Einwächter H. M., Haas H. G., Kern R. (1976): Calcium-sodium antagonism on the frog's heart: a voltage clamp study. J. Physiol. (London). **259**, 617—645

Bonke F. I. M. (1973): Passive electrical properties of atrial fibers of the rabbit heart. Pfluegers Arch. **339**, 1—15

Brown H. F., Noble D., Noble S. J. (1976): The influence of non-uniformity on the analysis of potassium currents in heart muscle. J. Physiol. (London). **258**, 615—629

Chapman R. A., Fry C. H. (1978): An analysis of the cable properties of frog ventricular myocardium. J. Physiol. (London). **283**, 263—282

Connor J., Barr L., Jakobsson E. (1975): Electrical characteristics of frog atrial trabeculae in the double sucrose-gap. Biophys. J. **15**, 1047—1067

De Boer R. W., Wolfrat J. C. (1979): Mathematical model of the double-sucrose-gap voltage-clamp method. Math. Biosci. **43**, 265—279

De Hemptinne A. (1976): Voltage clamp analysis in isolated cardiac fibres as performed with two different perfusion chambers for double sucrose gap. Pfluegers Arch. **363**, 87—95

De Mello W. C. (1975): Effect of intracellular injection of calcium and strontium on cell communication in heart. J. Physiol. (London). **250**, 231—245

Eisenberg R. S., Johnson E. A. (1970): Three-dimensional electrical field problems, in physiology. Progr. Biophys. Mol. Biol. **20**, 1—65

Fischmeister R. (1980): Etude du courant calcique lent sur les préparations multicellulaires. Aspect théorique de la détermination du potential d'inversion et de la conductance maximale. Thèse Doctorat Ingénieur, Orsay

Giles W., Noble S. J. (1976): Changes in membrane currents in bullfrog atrium produced by acetylcholine. J. Physiol. (London) **261**, 103—124

Goto M., Yatani A., Tsuda Y. (1978): Stabilizing effects of adenosine on the membrane currents and tension components of the bullfrog atrium. Jpn. J. Physiol. **28**, 611—625

Haas H. G., Brommundt G. (1980): Influence of intercellular clefts on potential and current distribution in a multifiber preparation. Biophys. J. **30**, 327—350

Horačkova M., Vassort G. (1979): Slow inward current and contraction in frog atrial muscle at various extracellular concentrations of Na and Ca ions. J. Mol. Cell. Card. **11**, 733—753

Jack J. J. B., Noble D., Tsien R. W. (1975): Electric Current Flow in Excitable Cells. Clarendon Press, Oxford

Jakobsson E., Barr L., Connor A. (1975): An equivalent circuit for small atrial trabeculae of frog. Biophys. J. **15**, 1068—1085

Johnson E. A., Lieberman M. (1971): Heart: excitation and contraction. Annu. Rev. Physiol. **33**, 479—532

Johnson, E. A., Sommer J. R. (1967): A strand of cardiac muscle. Its ultrastructure and the electrophysiological implications of its geometry J. Cell Biol. **33**, 103—129

Julian F. J., Moore J. W., Goldman D. E. (1962): Membrane potentials of lobster giant axon obtained by use of the sucrose-gap technique. J. Gen. Physiol. **45**, 1195—1216

Kass R. S., Siegelbaum S. A., Tsien R. W. (1979): Three-micro-electrode voltage clamp experiments in calf cardiac Purkinje fibres: is slow inward current adequately measured? J. Physiol. (London). **290**, 201—225

Kléber A. G. (1973): Effects of sucrose solution on the longitudinal tissue resistivity of trabecular muscle from mammalian heart. Pfluegers Arch. **345**, 195—205

Kohlhardt M., Mnich Z. (1978): Studies on the inhibitory effect of verapamil on the slow inward current in mammalian ventricular myocardium. J. Mol. Cell. Card. **10**, 1037—1052

Loewenstein W. R., Kanno Y., Socolar S. J. (1978): The cell-to-cell channel. Fed. Proc. **37**, 2645—2650

McGuigan J. A. S. (1974): Some limitations of the double sucrose gap, and its use in a study of the slow outward current in mammalian ventricular muscle. With an Appendix by J. A. S. McGuigan and R. W. Tsien. J. Physiol. (London) **240**, 775—806

Moore J. W., Ramon F., Joyner R. W. (1975): Axon voltage-clamp simulations: II. Double sucrose gap method. Biophys. J. **15**, 25—35

Nargeot J., Challice C. E., Tan K. S., Garnier D. (1978): Influence of metabolic inhibition by NaCN on electrical and mechanical activities of frog atrial fibers: studies using current and voltage clamp. J. Mol. Cell. Card. **10**, 469—485

New W., Trautwein W. (1972): Inward membrane currents in mammalian myocardium. Pfluegers Arch. **334**, 1—23

Payet M. D., Schanne O. F., Ruiz-Ceretti E., Demers J. M. (1978). Slow inward and outward currents of rat ventricular fibers under anoxia. J. Physiol. (Paris), **74**, 31—35

Peskoff A. (1979a): Electrical potential in three-dimensional electrically syncytial tissues. Bull. Math. Biol. **41**, 163—181

Peskoff A. (1979b): Electric potential in cylindrical syncytia and muscle fibers. Bull. Math. Biol. **41**, 183—192

Ramon F., Anderson N., Joyner R. W., Moore J. W. (1975): Axon voltage-clamp simulations: IV A multicellular preparation. Biophys. J. **15**, 54—69

Reuter H., Scholz H. (1977): A study of the ion selectivity and the kinetic properties of the calcium dependent slow inward current in mammalian cardiac muscle. J. Physiol. (London). **264**, 17—47

Rougier O., Vassort G., Stämpfli R. (1968): Voltage clamp experiments on frog atrial heart muscle with the sucrose-gap technique. Pflügers Arch. **301**, 91—108

Sauviat M. P. (1980): Effects of ervatamine chlorhydrate on cardiac membrane currents in frog atrial fibres. Brit. J. Pharmacol. **71**, 41—49

Schoenberg M., Fozzard H. A. (1979): The influence of intercellular clefts on the electrical properties of sheep cardiac Purkinje fibers. Biophys. J. **25**, 217—234

Tarr M., Trank J. W. (1971): Equivalent circuit of frog atrial tissue as determined by voltage clamp-unclamp experiments. J. Gen. Physiol. **58**, 511—522

Tarr M., Trank J. W. (1974): An assessment of the double sucrose-gap voltage clamp technique as applied to frog atrial muscle. Biophys. J. **14**, 627—642

Tarr M., Trank J. W. (1976): Limitations of the double sucrose gap voltage clamp technique in tension-voltage determinations on frog atrial muscle. Circ. Res. **39**, 106—112

Taylor R. E. (1963): Cable theory. In: Physical Techniques in Biological Research. (Ed. Nastuk) pp. 219—262, Academic Press, New York

Ten Eick R., Nawrath H., Mc Donald T., Trautwein W. (1976): On the mechanism of the negative inotropic effect of acetylcholine. Pflügers Arch. **361**, 207—213

Tomita T. (1966): Electrical responses of smooth muscle to external stimulation in hypertonic solution. J. Physiol. (London) **183**, 450—468

Trautwein W., Kuffler S. W., Edwards C. (1956): Changes in membrane characteristics of heart muscle during inhibition. J. Gen. Physiol. **40**, 135—145

Turin L., Warner A. (1977): Carbon dioxide reversibly abolishes ionic communication between cells of early amphibian embryo. Nature **270**, 56—57

Vassort G., Rougier O., Garnier D., Sauviat M. P., Coraboeuf E., Gargouïl Y. M. (1969): Effects of adrenaline on membrane inward currents during the cardiac action potential. Pfluegers Arch. **309**, 70—81

Ventura-Clapier R., Vassort G. (1980): Electrical and mechanical activities of frog heart during energetic deficiency. J. Muscle Res. Cell. Motil. **1**, 429—444

Weingart R. (1977): The actions of ouabain on intercellular coupling and conduction velocity in mammalian ventricular muscle. J. Physiol. (London). **264**, 341—365

Wojtczak J. (1979): Contractures and increase in internal longitudinal resistance of cow ventricular muscle induced by hypoxia. Circul. Res. **44**, 88—95

Received April 28, 1982 / Accepted May 24, 1982